## Title

Self-Enforcing Feedback Activation between BCL6 and Pre-B Cell Receptor Signaling Defines a Distinct Subtype of Acute Lymphoblastic Leukemia



## Journal

Cancer Cell, 27(3)

## ISSN

1535-6108

## Authors

Geng, Huimin
Hurtz, Christian
Lenz, Kyle B
et al.

## Publication Date

2015-03-01

## DOI

10.1016/j.ccell.2015.02.003

Peer reviewed

HHS Public Access

Author manuscript

*Cancer Cell*. Author manuscript; available in PMC 2016 March 09.

Published in final edited form as:

*Cancer Cell*. 2015 March 9; 27(3): 409–425. doi:10.1016/j.ccell.2015.02.003.

# Self-enforcing Feedback Activation between *BCL6* and Pre-B Cell Receptor Signaling Defines a Distinct Subtype of Acute Lymphoblastic Leukemia

**Huimin Geng**[1,18], **Christian Hurtz**[1,18], **Kyle B. Lenz**[2,3,18], **Zhengshan Chen**[1], **Dirk Baumjohann**[4], **Sarah Thompson**[2,3], **Natalya Goloviznina**[2,5], **Wei-Yi Chen**[6,7], **Jianya Huan**[2,5], **Dorian LaTocha**[3], **Erica Ballabio**[8], **Gang Xiao**[1], **Jae-Woong Lee**[1], **Anne Deucher**[1], **Zhongxia Qi**[1], **Eugene Park**[1], **Chuanxin Huang**[9], **Rahul Nahar**[1], **Soo-Mi Kweon**[1], **Seyedmehdi Shojaee**[1], **Lai N. Chan**[1], **Jingwei Yu**[1], **Steven M. Kornblau**[10], **Janetta J. Bijl**[11], **B. Hilda Ye**[12], **Mark Ansel**[4], **Elisabeth Paietta**[13], **Ari Melnick**[9], **Stephen P. Hunger**[14], **Peter Kurre**[2,5], **Jeffrey W. Tyner**[3,15], **Mignon L. Loh**[16], **Robert G. Roeder**[6], **Brian J. Druker**[3,17], **Jan. A. Burger**[10], **Thomas A. Milne**[8], **Bill H. Chang**[2,3,19], and **Markus Müschen**[1,19,*]

[1]Departments of Laboratory Medicine, University of California San Francisco, San Francisco, CA 94143, USA

[2]Division of Pediatric Hematology and Oncology, Department of Pediatrics, Oregon Health & Science University, Portland, OR 97239, USA

[3]Knight Cancer Institute, Oregon Health & Science University, Portland, OR 97239, USA

[4]Microbiology and Immunology, University of California San Francisco, San Francisco, CA 94143, USA

[5]Papé Family Pediatric Research Institute Oregon Health & Science University, Portland, OR 97239, USA

[6]Laboratory of Biochemistry and Molecular Biology, the Rockefeller University, New York, NY 10065, USA

[*]Correspondence: Markus Müschen, Department of Laboratory Medicine, University of California San Francisco, 513 Parnassus Ave, San Francisco CA 94143, markus.muschen@ucsf.edu.

[18]Co-first authors;

[19]Co-senior authors

**ACCESSION NUMBERS**

The gene expression microarray and ChIPseq data reported in this paper have been deposited in the NCBI Gene Expression Omnibus (GEO) (http://www.ncbi.nlm.nih.gov/geo) database with the GEO accession numbers GSE59332 and GSE59538.

SUPPLEMENTAL INFORMATION

Supplemental Information including Supplemental Experimental Procedures, six Figures and eight Tables can be found with this article online.

**AUTHOR CONTRIBUTIONS**

H.G., C.H. and K.B.L. designed and performed the majority of the analysis and experiments. Z.C., D.B., S.T., N.G., W.Y.C., J.H., D.L, E.B., G.X., J.L., A.D., Z.Q., E.P., C.H., R.N., S.M.K., S.S., L.N.C., J.Y., J.W.T., B.H.C., S.M.K. and T.A.M. performed experiments and analyzed data. H.G., A.D., S.M.K., E.P., A.M., S.P.H., M.L.L. and B.H.C. provided and characterized patient samples and clinical outcome data. J.J.B., B.H.Y., M.A., A.M., J.A.B., R.G.R. and M.M. provided important reagents and mouse samples. M.M. and B.H. designed experiments and conceived the study. M.M. wrote the paper.

[7]Institute of Biochemistry and Molecular Biology, National Yang-Ming University, Taipei, Taiwan

[8]MRC Molecular Haematology Unit, Weatherall Institute of Molecular Medicine, University of Oxford, Oxford, OX3 9DS, UK

[9]Departments of Medicine and Pharmacology, Weill Cornell Medical College, New York, NY 10065, USA

[10]Department of Leukemia, the University of Texas M.D. Anderson Cancer Center, Houston, TX 77030, USA

[11]Hôpital Maisonneuve-Rosemont, Montreal, QC H1T 2M4, Canada

[12]Department of Cell Biology, Albert Einstein College of Medicine, Bronx, NY 10461, USA

[13]Department of Medicine, Albert Einstein College of Medicine, Bronx, NY 10461, USA

[14]Division of Pediatric Oncology and Center for Childhood Cancer Research, Children's Hospital of Philadelphia, Philadelphia, PA 19104, USA

[15]Department Cell & Developmental Biology, Oregon Health & Science University, Portland, OR 97239, USA

[16]Pediatric Hematology-Oncology, University of California San Francisco, San Francisco, CA 94143, USA

[17]Howard Hughes Medical Institute, Portland, OR 97239, USA

## SUMMARY

Studying 830 pre-B ALL cases from four clinical trials, we found that human ALL can be divided into two fundamentally distinct subtypes based on pre-BCR function. While absent in the majority of ALL cases, tonic pre-BCR signaling was found in 112 cases (13.5%). In these cases, tonic pre-BCR signaling induced activation of BCL6, which in turn increased pre-BCR signaling output at the transcriptional level. Interestingly, inhibition of pre-BCR-related tyrosine kinases reduced constitutive BCL6 expression and selectively killed patient-derived pre-BCR$^+$ ALL cells. These findings identify a genetically and phenotypically distinct subset of human ALL that critically depends on tonic pre-BCR signaling. *In vivo* treatment studies suggested that pre-BCR tyrosine kinase inhibitors are useful for the treatment of patients with pre-BCR$^+$ ALL.

## INTRODUCTION

Bone marrow progenitor cells in mice produce approximately 10 million pre-B cells daily (Osmond, 1991), the vast majority of which is eliminated at the pre-B cell receptor (BCR) checkpoint (Sakaguchi and Melchers, 1986). Early pre-B cells are programmed to die unless they productively rearrange $V_HDJ_H$ gene segments and are rescued by 'tonic' pre-BCR signal activity into the long-lived pool of mature peripheral B cells (Rajewsky, 1996). Even in mature B cells, continuous tonic signaling from the BCR is required for B cell survival and maintenance and conditional ablation of tonic BCR signaling results in rapid B cell depletion (Kraus et al., 2004). Interestingly, however, loss of tonic BCR signaling can be rescued by activation of PI3K-AKT signaling (Srinivasan et al., 2009), identifying PI3K-

AKT as a central survival pathway downstream of the (pre-) BCR. Tonic pre-BCR signaling involves constitutive activity of the proximal pre-BCR-associated SRC family kinases LYN, FYN and BLK (Saijo et al., 2003) as well as SYK and ZAP70 (Schweighoffer et al., 2003), which then activate PI3K (Guo et al., 2000; Okada et al., 2000). Recent work highlighted the particular importance of the PI3K p110δ (PIK3CD) isoform for pre-BCR survival signaling during early B cell development (Ramadani et al., 2010). The discovery that most subtypes of B cell lymphoma critically depend on BCR signaling (Davis et al., 2010; Schmitz et al., 2012) has led to the development of new targeting strategies that focus on BCR signaling at the level of SRC kinases (Lyn, Fyn and Blk), SYK/ZAP70 and PI3Kδ (Burger and Okkenhaug, 2014; Chen et al., 2006; Chen et al., 2013; Cheng et al., 2011; Ke et al., 2009; Yang et al., 2008). In addition, small molecule inhibition of BTK, which mediates 'chronic active BCR signaling' in activated B cell-like (ABC) diffuse large B cell lymphoma (DLBCL), chronic lymphocytic leukemia (CLL) and mantle cell lymphoma (MCL) has achieved major clinical success in the treatment of these diseases (Byrd et al., 2013; Davis et al., 2010; Schmitz et al., 2012; Wang et al., 2013). While the role of BCR signaling in the biology and treatment has been elucidated in all major B cell lymphoma subtypes, the role of pre-BCR signaling has not been systematically studied in human pre-B acute lymphoblastic leukemia (ALL).

Goals of the present study were (i) to identify cases of human pre-B ALL with tonic or chronic active pre-BCR signaling, (ii) to estimate their frequency, (iii) to determine the role of pre-BCR signaling in specific pre-B ALL subtypes, (iv) to identify cooperating genetic lesions and (v) to develop a concept for therapeutic targeting of the pre-BCR pathway in human pre-B ALL.

## RESULTS

### Expression and Activity of the pre-BCR Defines a Distinct Subtype of Human ALL

To elucidate pre-BCR expression and function in pre-B ALL cells, we measured expression of the immunoglobulin μ heavy chain (μHC), and the pre-BCR surrogate light chain components λ5 (IGLL1) and VpreB on a series of 31 patient-derived pre-B ALL xenograft samples and 15 ALL cell lines by flow cytometry (Table S1–S3). 28 of the 46 pre-B ALL samples and cell lines tested lacked surface pre-BCR expression including 5 *MLL*-rearranged (*MLLr*), 16 *BCR-ABL1*, 2 *ETV6-RUNX1*, and 5 ALL with other abnormalities. Of the 18 pre-BCR$^+$ ALL cases, 14 harbored a *PBX1* gene rearrangement (1q23), one carried a deletion at 6q21, one carried both *PBX1* gene rearrangement and 6q21 deletion and two harbored *PDGFRB* gene rearrangements (Figure 1A–1B and S1A–S1I). Engagement of the pre-BCR using μHC-specific antibodies resulted in strong $Ca^{2+}$ mobilization from cytoplasmic stores in all 7 pre-BCR$^+$ ALL cases tested but not in any of the 19 other cases (Figure 1C and S1A–S1I). These findings suggest that most cases of human ALL lack pre-BCR signaling (pre-BCR$^-$), whereas a distinct ALL subgroup (pre-BCR$^+$) exists that is defined by pre-BCR expression and activity. Indeed, key components of the pre-BCR signaling, including SRC family kinases (LYN, BLK), SYK, BTK and PLCγ2 were constitutively active in 6 pre-BCR$^+$ ALL samples (Figure 1D). Interestingly,

phosphorylation of these molecules was sensitive to treatment of the dual ABL1/SRC-BTK inhibitor Dasatinib (Figure 1D).

## Tonic pre-BCR Signaling including Activation of SRC, SYK and PI3K in a Subset of Human ALL

To compare baseline signaling activity of pre-BCR$^-$ and pre-BCR$^+$ ALL cells in a large cohort of patients (MDACC 1983–2007; n=208), we divided patient samples into two groups based on flow cytometry measurements of pre-BCR (μHC) expression and the Igα signaling chain CD79A (Figure S1J). None of the pre-BCR$^+$ ALL cases in this cohort (n=26) expressed the stem/progenitor cell antigen CD34 and CD25, which are both expressed on the surface of most of the 182 pre-BCR$^-$ ALL cases (Figure S1K). Using a panel of 133 validated antibodies, we interrogated those 208 pre-B ALL samples at the time of diagnosis for expression and activity of 66 signaling molecules on reverse phase protein arrays (RPPA) (Tibes et al., 2006). RPPA analyses revealed that pre-BCR$^+$ ALL cells exhibit significantly higher expression and activity of SRC family kinases including LYN, and strong constitutive activity of multiple components of the PI3K-AKT pathway, including PIK3R1 (p85α), PIK3CD (p110δ), AKT1-pS$^{473}$/T$^{308}$, MTOR-pS$^{2448}$, RPS6KB-pS$^{371}$ and RPS6-pS$^{235}$/S$^{236}$ (Figure 1E and S1L). Consistent with strong PI3K-AKT signaling, expression and activity of PTEN, a negative regulator of PI3K-AKT signaling, is low in pre-BCR$^+$ ALL cells. These findings are consistent with the established central role of SRC/LYN kinase (Saijo et al., 2003) and PI3K-AKT signaling (Srinivasan et al., 2009), in particular PIK3d (Ramadani et al., 2010), in tonic pre-BCR signaling. Pre-BCR$^+$ ALL cases are also distinct from pre-BCR$^-$ ALL cases by particularly low levels of STAT5 expression and activity (Figure S1L). We conclude that pre-BCR$^+$ ALL cells are defined by a distinct signaling phenotype including constitutive SRC and PI3K-AKT signaling and lack of STAT5 activity.

## Tonic pre-BCR Signaling Is Associated with a Distinct Gene Expression Profile in Human ALL

Upregulation of tonic pre-BCR signaling at the expense of STAT5 in pre-B ALL is reminiscent of negative regulation of IL7R/STAT5 upon pre-BCR activation during normal early B cell development (Ochiai et al., 2012). The shift from IL7R/STAT5 to pre-BCR signaling during early B cell differentiation triggers profound gene expression changes. Therefore, we analyzed the gene expression data from 3 pre-B ALL clinical trials for children (COG P9906, n =207 (Harvey et al., 2010) and St. Jude Research Hospital, n=132 (Ross et al., 2003)) and adults (ECOG E2993, n=191 (Geng et al., 2012)). Patients in these trials were classified as pre-BCR$^-$ or pre-BCR$^+$ based on pre-BCR expression (*IGLL1*, *IGLL3*, *VPREB1*, *VPREB3*, *IGHM*) and its associated signaling molecules *SYK* and *ZAP70* (Figure 2A–2C). To identify a common gene expression signature for pre-BCR$^+$ ALL, we performed a supervised analysis of the microarray data and identified a set of 40 genes concordantly differentially expressed in pre-BCR$^+$ vs. pre-BCR$^-$ ALL in all 3 clinical cohorts (Figure 2A–2C). The up-regulated genes include pre-BCR signaling molecules (*PRKCZ*, *BLNK*, *BLK*, *LYN*, *MERTK*, *ROR1*) and transcription factors that promote B-cell differentiation (*BCL6*, *BACH2*, *IRF4*, *TCF3*, *POU2AF1*). Down-regulated genes include *IL2RA* (CD25) and CD34, confirming flow cytometry data from the MDACC cohort (Figure

S1K), the STAT5 target genes (*ID2*, *CD69*, *CD99*, *ITGA6*, *CCND2*, *SOCS2*) and *PRDM1* (BLIMP1) (Figure 2A–2C).

## Frequent Rearrangement of PBX1 in pre-BCR$^+$ ALL

We studied the coding capacity of immunoglobulin heavy chain $V_HDJ_H$ gene rearrangements in 152 primary pre-B ALL samples and normal B cell precursors as reference (Trageser et al., 2009). Human bone marrow pro-B, pre-B and immature B cells from healthy donors (n=2) were studied by single-cell PCR. In marked contrast to other pre-B ALL subsets, most cases with *TCF3-PBX1* rearrangement and/or 6q21 deletion carried productively rearranged *IGHM* alleles and showed evidence of selection for expression of in-frame $V_HDJ_H$ gene rearrangements, like normal pre-B cells (Figure 2D–2E; Table S4). In contrast, productive $V_HDJ_H$ gene rearrangements were negatively selected in all other ALL subsets. Combining data from 4 clinical trials (n=830, Table S5), we collectively found evidence of pre-BCR function in 112 cases (13.5%). Pre-BCR expression was frequent among ALL cases with *PBX1*-rearrangement or -duplication and 6q21 deletion, but rare or absent in cases with *MLLr*, *BCR-ABL1*, *ETV6-RUNX1* and hyperdiploid ALL (Figure 2F; Table S5–S6).

## TCF3-PBX1 Binds to and Upregulates pre-BCR Genes in Human ALL Cells

*PBX1* is a proto-oncogene with a critical role in hematopoiesis and lymphopoiesis (Sanyal et al., 2007). In pre-B ALL, *PBX1* (1q23) is frequently rearranged to the B cell-specific *TCF3* (19p13) locus, encoding E2A (E12 and E47) transcription factors. In these cases, the N-terminal transcriptional activation domains of TCF3 (exons 1–16, $TCF3^N$) are fused to the C-terminal Hox cooperative motif and homeodomain of PBX1 (exons 4-9, $PBX1^C$) (Nourse et al., 1990). To identify targets of oncogenic TCF3-PBX1 activity, we performed chromatin immunoprecipitation (ChIP), followed by massively parallel DNA sequencing (ChIPseq), using antibodies against the $PBX1^C$, the $TCF3^N$ and the TCF3-PBX1 co-activator p300 (Bayly et al., 2004) in a *TCF3-PBX1* ALL cell line (697) and a primary *TCF3-PBX1* ALL sample (ICN12) (Figure S2A). ChIPseq data revealed that TCF3-PBX1, in concert with its coactivator p300, strongly bound to promoter regions of genes that encode key components of the pre-BCR, including *IGLL1*, *VPREB1*, *VPREB3*, *CD79A* and *CD79B*, as well as μHC enhancer regions (Figure 3A). Specific binding of TCF3-PBX1 to these 6 loci was confirmed by single-locus quantitative ChIP (qChIP), using the fusion-specific TCF3-PBX1-hf (Figure 3B and S2B) and the $TCF3^N$, $PBX1^C$ and p300 antibodies (Figure S2C–S2F). To identify genome-wide target genes that are directly regulated by *TCF3-PBX1*, we matched TCF3-PBX1 binding (ChIPseq, Figure S2D–S2F) with specific gene expression changes that distinguish *TCF3-PBX1* cases from other pre-B ALL subsets (Ross et al., 2003). Among the 1,343 TCF3-PBX1 ($PBX1^C$, $TCF3^N$ and p300) target genes in promoter regions (within 2kb distance from transcription start site), 99 were specifically up-regulated, including multiple pre-BCR components (*IGLL1*, *VREB1*, *VREB3*, *IGHM*) and pre-BCR downstream signaling molecules (*BLK*, *LCK*, *SYK*, *ZAP70*, *PIK3CD*, *PIK3R1*). In addition, 111 targets were significantly downregulated in *TCF3-PBX1* compared to other pre-B ALL subtypes, including the STAT5 target genes *CD69* and *SOCS2* (Figure 3C–3D). A pathway analysis of TCF3-PBX1 ChIPseq/gene expression targets suggested that TCF3-PBX1 is a

positive regulator of B cell development and BCR signaling and negatively regulated STAT5 (Figure 3E).

To further test whether gene rearrangement and oncogenic activation of *TCF3-PBX1* induces pre-BCR activity, we studied full-blown ALL populations that had developed after latencies of 90–180 days in the bone marrow from the *TCF3-PBX1*-, *BCR-ABL1*- and *MLL-AF4*-transgenic mice. Flow cytometry of surface μHC and CD79B (Igβ) expression confirmed that ALL cells developing in *TCF3-PBX1*-transgenic mice are characterized by pre-BCR expression in contrast to pre-BCR$^-$ ALL in *BCR-ABL1*-and *MLL-AF4*-transgenic mice (Figure 3F).

## Pre-BCR Signaling Regulates the Balance between BCL6 and STAT5 Activity in Human ALL

Studying gene expression changes in 530 ALL cases from 3 clinical trials (St Jude, COG P9906, ECOG E2993; Table S5), we found that pre-BCR$^+$ ALL cells (n=71, 13.4%) exhibit consistently higher expression levels of BCL6 than pre-BCR$^-$ cases (n=459, 86.4%; Figure 2A–2C). Quantitative RT-PCR analyses confirmed 6- to 30-fold higher mRNA and protein levels of *BCL6* in *TCF3-PBX1* ALL compared to other ALL subsets (Figure 4A and S3A). These findings suggested that BCL6 may be a direct target of TCF3-PBX1 and other oncogenic transcription factors that drive pre-BCR$^+$ ALL. However, ChIPseq and qChIP analysis showed no evidence of binding of TCF3-PBX1 to the *BCL6* locus (Figure S3B–S3C), indicating that TCF3-PBX1 induces BCL6 expression through an indirect mechanism. Recent studies by us and others (Duy et al., 2010; Swaminathan et al., 2013) revealed a critical role of BCL6 as a survival factor at the pre-BCR checkpoint during normal B cell development. In *BCR-ABL1* ALL (pre-BCR$^-$), inhibition of STAT5 activity by treatment with tyrosine kinase inhibitors induced strong expression of BCL6 (Duy et al., 2011). Likewise, in our Western blot analysis, while pre-BCR$^+$ (*TCF3-PBX1*) ALL cases expressed high levels of BCL6 in the absence of STAT5 activity, we observed the converse in pre-BCR$^-$ (*BCR-ABL1*) ALL cells (Figure 4A). To test whether pre-BCR signaling directly affects the balance between BCL6 and STAT5, we used an inducible system for pre-BCR activation in mouse ALL cells. To this end, *Rag2*$^{-/-}$ mouse ALL cells, lacking the ability of endogenous pre-BCR expression, were engineered to express a pre-rearranged tetracyclin-inducible μHC, which results in subsequent pre-BCR expression (Trageser et al., 2009). Inducible pre-BCR activation resulted in a massive increase of BCL6 protein levels (40-fold) and concomitant silencing of STAT5 activity (p-Y$^{694}$; Figure 4B). Similarly, complementation of a defective pre-BCR signaling chain in *Blnk*$^{-/-}$ or *Ighm*$^{-/-}$ mouse ALL cells by reconstitution of Blnk or μHC-expression caused dramatic upregulation of BCL6 at the expense of STAT5 activity (p-Y$^{694}$; Figure 4B). Likewise, Cre-mediated deletion of Stat5 in *Stat5a/b*$^{fl/fl}$ ALL cells was sufficient to increase BCL6 protein levels (Figure 4C). These experiments provide genetic evidence that the balance between BCL6 and STAT5-activity is directly influenced by pre-BCR signaling and, hence, suggests that high expression levels of BCL6 represent as a surrogate marker for pre-BCR activity in human ALL cells.

## BCL6 Expression Represents a Surrogate Marker for pre-BCR Activity in Human ALL

Immunohistochemical analyses for expression of the pre-BCR (μHC) and BCL6 were performed on bone marrow biopsies from 72 ALL patients. These analyses confirmed that all 12 pre-BCR$^+$ (μHC$^+$) ALL cases express BCL6 at high levels (Figure S3D; Table S7). These cases carried lesions affecting *PBX1*, through *TCF3-PBX1* and/or gain of 1q23 encompassing *PBX1*. By contrast, 60 other cases lacked both BCL6 and μHC surface expression (Figure S3E). We next performed double-stainings for BCL6 and μHC on the same slides, confirming that pre-BCR$^-$ ALL cells express neither μHC nor BCL6. In pre-BCR$^+$ ALL cases, virtually all ALL cells expressed both surface μHC and BCL6 at levels comparable to mature B cell lymphoma carrying *IGH-BCL6* rearrangement (Figure 4D). Bone marrow biopsies from pre-BCR$^+$ ALL cases included various degrees of admixtures of normal bone marrow cells that lacked both μHC and BCL6 expression.

## SYK Tyrosine Kinase Signaling Is Required for BCL6 Activation downstream of Tonic pre-BCR Signaling

Based on the finding that BCL6 is induced by pre-BCR signaling and is a potential target for drug-treatment in pre-BCR$^+$ ALL cells, we measured the effects of small molecule inhibitors of proximal pre-BCR tyrosine kinases on BCL6 expression. While 57 of 61 ALL cases with *PBX1*-rearrangement or duplication showed evidence of tonic pre-BCR signaling (Figure 2F; Table S5), we did not find pre-BCR activity in any of 196 cases with *Ph*$^+$ ALL (*BCR-ABL1*). Consistent with divergent pre-BCR activity in these subsets, we found that *TCF3-PBX1* but not *BCR-ABL1* fusion oncogenes induced expression of BCL6 in pre-B ALL cells (Figure 4E). Treatment with small molecule tyrosine kinase inhibitors of SYK (PRT062607) and BTK (Ibrutinib) reduced BCL6 expression in pre-BCR$^+$ *TCF3-PBX1* ALL cells (Figure 4F and 4G), demonstrating that SYK tyrosine kinase activity is required for BCL6 expression in pre-BCR$^+$ ALL cells. While *TCF3-PBX1* induces constitutive BCL6 expression via tonic pre-BCR signaling, *BCR-ABL1* represses BCL6 expression. *Ph*$^+$ ALL lack BCL6 expression in the presence of active BCR-ABL1, however, ABL1 tyrosine kinase inhibitors (Nilotinib, Dasatinib) relieve BCR-ABL1/STAT5-mediated repression of BCL6 (Figure 4H). Interestingly, the specific ABL1 kinase inhibitor Nilotinib, which does not affect pre-BCR signaling, has no effect on constitutive BCL6 expression in *TCF3-PBX1* ALL cells. However, the dual ABL1/SRC kinase inhibitor Dasatinib, which inhibits the SRC kinases BLK, LYN and FYN upstream of SYK, almost entirely abolished BCL6 expression in pre-BCR$^+$ *TCF3-PBX1* ALL cells (Figure 4H). These findings reveal that based on divergent functions of pre-BCR/BCL6 signaling, human ALL can be divided into two genetically and phenotypically distinct subsets.

We propose that in the majority of ALL cases, the transforming oncogene (e.g. *BCR-ABL1*) mimics constitutive active cytokine signaling via activation of STAT5 and repression of BCL6. In 10–15% of the cases, oncogenic lesions (e.g. *TCF3-PBX1;* Table S8) result in tonic pre-BCR signaling and activation of BCL6. These differences may reflect different cells of origins of the two subsets. BCR-ABL1 engages IL7R-dependent survival and proliferation signals via STAT5 that are active in pro-B and early pre-B cells (Fraction C); by contrast, activation of pre-BCR signaling (e.g. by *TCF3-PBX1*) in late pre-B cells (Fraction C′) suppresses IL7R and cytokine signaling (Ochiai et al., 2012). We propose that

the mutually exclusive nature of cytokine receptor/STAT5 and pre-BCR/BCL6 pathways in human ALL reflects distinct developmental origins from early (Fraction C) and late (Fraction C′) pre-B cells (Figure 4I). BCL6 ChIPseq analysis revealed that BCL6 and STAT5 binding sites were the most highly enriched DNA elements ($p=10^{-60}$ for both) associated with BCL6 binding peaks in *TCF3-PBX1* ALL cells (Figure 4I), suggesting that BCL6 and STAT5 may compete for binding to those promoters, which would be consistent with mutual exclusive activity of STAT5 and BCL6 in pre-BCR$^-$ and pre-BCR$^+$ ALL subtypes, respectively.

## Genetic Mouse Model of Conditional BCL6 Ablation in pre-BCR$^+$ TCF3-PBX1 ALL

BCL6 functions as a classical proto-oncogene in germinal center-derived B cell lymphoma (Ye et al., 1993) and represents a powerful survival factor at the pre-BCR checkpoint during early B cell development (Duy et al., 2010). For these reasons, we developed a genetic mouse model to determine the role of BCL6 in pre-BCR$^+$ ALL cells. In *Bcl6*$^{fl/fl}$-mCherry mice, exons 5–10 were flanked by *Lox*P sites and Cre-mediated deletion of these exons results in expression of a truncated Bcl6 protein fused to mCherry (Figure 5A). Thereby mCherry expression reflects transcriptional activity of the *Bcl6* promoter and Cre-mediated deletion can be used for inducible ablation of Bcl6 function and as mCherry-based reporter of Bcl6 expression. In a genetic experiment, we transduced *Bcl6*$^{fl/fl}$-mCherry pre-B cells with *TCF3-PBX1* or an empty vector (EV) control. Cre-mediated deletion (Figure 5B) activated the *Bcl6*-mCherry reporter (Figure 5C). While only ~1% of pre-B cells carrying an EV control showed transcriptional activation of the *Bcl6* promoter, more than 50% of *TCF3-PBX1*-transduced cells actively transcribed *Bcl6* (Figure 5C). These findings demonstrate that TCF3-PBX1 indirectly induces Bcl6 expression through transcriptional activation of pre-BCR signaling.

## BCL6 Transcriptionally Activates pre-BCR Components in TCF3-PBX1 ALL

To identify BCL6 transcriptional targets in pre-BCR$^+$ ALL cells, we performed ChIPseq analysis in patient-derived *TCF3-PBX1* ALL cells (Figure S4A–S4D). As in DLBCL and *Ph*$^+$ ALL (Duy et al., 2011), BCL6 directly binds to a number of checkpoint molecules including *RB1*, *CDKN2C* and *CDKN1B* in pre-BCR$^+$ ALL (Figure S4A). A previous study demonstrated that BCL6 increases tonic BCR signaling in DLBCL cells by transcriptional repression of the inhibitory phosphatase *PTPRO* (Juszczynski et al., 2009). Likewise, *PTPRO* was also identified as a transcriptional target of BCL6 in pre-BCR$^+$ ALL cells. In addition, BCL6 also binds to pre-BCR components (*IGLL1*, *VPREB1*) and downstream signaling molecules (*BLK*, *BANK1*, *SYK*) (Figure 5D). QChIP validated BCL6 binding to these loci (Figure S4B). To determine how BCL6 binding affects gene expression in *PBX1*-rearranged ALL cells, we measured gene expression changes in response to acute ablation of Bcl6 in a *Bcl6*$^{fl/fl}$-mCherry mouse model for *TCF3-PBX1* ALL. Upon Cre-mediated deletion of *Bcl6*, multiple BCL6 target genes were de-repressed, including checkpoint molecules *RB1*, *CDKN1A*, *CDKN1B*, *CDKN2A* and *CDKN2C* (Figure 5E and 5F). Also *PTPRO* were among the de-repressed BCL6 target genes, suggesting that BCL6 increases tonic pre-BCR signaling by transcriptional repression of the (pre-)BCR signaling inhibitor *PTPRO* as described in DLBCL (Juszczynski et al., 2009). Interestingly, BCL6 targets with transcriptional activation by Bcl6 include multiple pre-BCR related molecules (*Bank1*, *Syk*;

Figure 5E and 5F). To test BCL6-dependent gene regulation in ALL patient samples, we integrated BCL6 ChIPseq target genes with a BCL6-dependent signature of gene expression in 118 cases of childhood pre-B ALL (St. Jude). This analysis showed transcriptional activation of 63 BCL6 target genes including multiple pre-BCR related molecules (*IGLL1*, *BLK*, *VPREB1*, *PIK3CD*, *SYK*; Figure 5G and 5H). Collectively, these findings suggest a self-enforcing activation loop between tonic pre-BCR signaling and BCL6 activity in a subset of human ALL: Oncogenic activation of tonic pre-BCR signaling (e.g. as a result of *PBX1*-rearrangement and –duplication) induces strong activation of BCL6, which further activates pre-BCR signaling (e.g. through transcriptional repression of *PTPRO* and *PRDM1* and activation of *IGLL1*, *VPREB1*, *BLK*, *SYK*). Interestingly, PBX1 binding to promoter regions of pre-BCR-related genes frequently co-localizes with binding of BCL6, suggesting that BCL6 and PBX1 cooperate in the regulation of these genes (Figure 5I).

## Pre-BCR$^+$ ALL Cells Are Dependent on BCL6-Activity

Pre-BCR$^+$ ALL and BCR-dependent B cell lymphoma share constitutively high BCL6 expression levels. To determine whether high expression levels of BCL6 correlate with clinical outcome of ALL patients, we analyzed mRNA levels of *BCL6* at the time of diagnosis in children with high-risk ALL (COG P9906) and adults with ALL (ECOG E2993). Only patients of known pre-BCR expression status were included in the analysis. Since BCL6 was specifically upregulated by tonic pre-BCR signaling, we performed clinical outcome analyses separately for pre-BCR$^+$ and pre-BCR$^-$ ALL cases. In both the pediatric (COG P9906; p=0.043) and adult (ECOG E2993; p=0.013) clinical trials, higher than median expression levels of BCL6 were predictive of poor outcome among patients with pre-BCR$^+$ but not pre-BCR$^-$ ALL (Figure 6A and 6B). These findings suggest that high expression levels of BCL6 affect the course of disease in pre-BCR$^+$ but not pre-BCR$^-$ ALL. To determine the potential contribution of BCL6 signaling to survival and proliferation of pre-BCR$^+$ ALL cells, we studied inducible ablation of *Bcl6* in a mouse model (Figure 5A–5C). *Bcl6*$^{fl/fl}$ *TCF3-PBX1* ALL cells were transduced with 4-hydroxy-tamoxifen (4-OHT)-inducible Cre (Cre-ER$^{T2}$) or an EV control (ER$^{T2}$). While 4-OHT mediated deletion of *Bcl6* resulted in progressive depletion of Cre-ER$^{T2}$-transduced cells, it had no measurable effects in ER$^{T2}$-transduced *Bcl6*$^{fl/fl}$ *TCF3-PBX1* ALL cells (Figure 6C). To verify BCL6-dependency of pre-BCR$^+$ ALL in a patient-derived setting, we transduced xenografted *TCF3-PBX1* ALL cells with an inducible dominant-negative BCL6 mutant lacking the BCL6-BTB domain ($^{DN}$BCL6-ER$^{T2}$) (Shaffer et al., 2000). While the fraction of ICN12 cells carrying ER$^{T2}$ empty vectors remained stable after 4-OHT treatment, cells transduced with $^{DN}$BCL6-ER$^{T2}$ were rapidly depleted (Figure 6D). These findings collectively identify BCL6 as a potential target for the treatment of pre-BCR$^+$ ALL.

## Pharmacological Inhibition of BCL6 in pre-BCR$^+$ ALL Cells

In a complementary approach, we tested the consequences of shRNA-mediated knockdown of BCL6 in pre-BCR$^+$ ALL cells. Upon doxycycline-inducible expression of BCL6-specific shRNAs, we observed moderate reduction of BCL6 protein expression and impaired colony formation capacity in pre-BCR$^+$ ALL cells (Figure S5A–S5C). For proof-of-principle experiments, a specific *retro-inverso* BCL6 peptide-inhibitor (RI-BPI) was used to inhibit BCL6 function (Cerchietti et al., 2009). Treatment of patient-derived pre-BCR$^+$ ALL cells

with 5 μmol/l RI-BPI induced cell cycle arrest within 1 day of treatment (Figure 6E and S5D) and caused impaired colony formation capacity (Figure S5E). Whereas RI-BPI treatment alone did not induce significant acute toxicity, it strongly sensitized pre-BCR$^+$ ALL cells to Vincristine (1 nmol/l; p=0.003; Figure 6F and S5F), a mitotic spindle inhibitor that is part of the chemotherapy backbone in most current clinical trials for ALL. In conclusion, BCL6 represents a predictor of poor clinical outcome and a potential target for therapy of patients with pre-BCR$^+$ ALL.

## Pre-BCR$^+$ and pre-BCR$^-$ ALL Cells Exhibit Distinct Kinase-Inhibitor Sensitivity Profiles

Besides inhibition of BCL6 expression (Figure 4F–4H and S6A), PRT062607 (SYK), Ibrutinib (BTK) and Dasatinib (SRC) induced selective toxicity in pre-BCR$^+$ ALL cells (Figure 7A). Pre-BCR$^+$ ALL (n=7), pre-BCR$^-$ ALL (n=8) and mature B cell lymphoma cells (n=2) were treated with inhibitors of pre-BCR tyrosine kinases PRT062607 (SYK), Ibrutinib (BTK), Dasatinib (SRC) as well as inhibitors of pre-BCR downstream signaling, including GS-1101 (PI3Kδ), AZD05363 (AKT1), Rapamycin (mTOR), AZD6244 (MEK1), SCH772984 (ERK1, ERK2), Enzastaurin (PKCβ), MI2 (MALT1) and BMS345541 (IKK, NF-κB) (Figure S6B). For treatment with the dual SRC/ABL1 kinase inhibitor Dasatinib, only *Ph*$^+$ ALL cells expressing mutant *BCR-ABL1*$^{T315I}$ were studied to rule out effects of BCR-ABL1 tyrosine kinase inhibition. Compared to pre-BCR$^-$ ALL and mature B cell lymphoma cells, pre-BCR$^+$ ALL cells were selectively sensitive to inhibition of SYK and SRC (BLK, LYN) and, to some lesser degree, to inhibition of BTK (Figure 7A) and PI3Kδ (Figure S6B). On the other hand, pre-BCR$^-$ ALL cells were selectively sensitive to inhibitors of MEK1 (AZD6244) and ERK1/2 (SCH772984), suggesting that pre-BCR$^+$ and pre-BCR$^-$ ALL cells can be distinguished based on a specific profile of kinase-inhibitor sensitivity.

To address this possibility in a formal experiment, we treated pre-BCR$^+$ (n=8) and pre-BCR$^-$ (n=9) ALL cells with a diverse panel of 51 kinase inhibitors that are currently being studied for the treatment of hematological malignancies and solid tumors (Figure 7B). This analysis confirmed that pre-BCR$^+$ ALL cells are particularly sensitive to inhibitors of SYK, SRC and PIK3δ, whereas pre-BCR$^-$ ALL cells are more responsive to inhibition of MEK1 and ERK1/2 (Figure 7B). Integrating experimentally measured sensitivities to individual inhibitors with their known biochemical $IC_{50}$ values for individual kinase targets, we established a kinase dendrogram of specific vulnerabilities of pre-BCR$^+$ and pre-BCR$^-$ ALL (Figure 7C). While pre-BCR$^+$ ALL cells were most dependent on SYK, ZAP70, BTK, and LYN activity, pre-BCR$^-$ ALL cells were most vulnerable to inhibition of ABL1, PDGFR, ERK1, ERK2, MET and KIT kinase activity (Figure 7C).

## Validation of pre-BCR-BCL6 Signaling as Therapeutic Target in pre-BCR$^+$ ALL Cells

The usefulness of pre-BCR signaling inhibitors PRT062607 (SYK), Ibrutinib (BTK) and Dasatinib (SRC, BTK) for the treatment of pre-BCR$^+$ ALL was tested in a proof-of-principle experiment. To this end, one million patient-derived *TCF3-PBX1* pre-BCR$^+$ ALL cells (ICN12) labelled with luciferase were injected intravenously into sublethally irradiated NOD/SCID mice. Recipient mice were then treated with vehicle (n=11), PRT062607 (100 mg/kg; n=7), Ibrutinib (75 mg/kg; n=7) and Dasatinib (40 mg/kg; n=12). All the inhibitors

were well tolerated and achieved significant reduction of leukemia burden *in vivo*, as determined by luciferase bioimaging (Figure 8A). These experiments, together with *in vitro* testing (Figure 7A and 7B) suggested that Dasatinib has the strongest anti-leukemic effect among the 3 pre-BCR signaling inhibitors. For this reason, we prioritized Dasatinib for detailed *in vitro* validation experiments for a group of 135 patient-derived ALL samples, including various ALL subtypes but not $Ph^+$ ALL. Patient-derived ALL cells were cultured over 72 hr in the absence or presence of Dasatinib in concentrations ranging from 1 nmol/l to 1,000 nmol/l to calculate Dasatinib $IC_{50}$ values for these cases. Our previous kinase inhibitor screening assays (Tyner et al., 2013) showed that the median $IC_{50}$ for Dasatinib of all hematologic malignancy samples received at OHSU (n>400) was 900 nmol/l. Importantly, all 22 pre-$BCR^+$ ALL cases were sensitive to Dasatinib ($IC_{50}$<50 nmol/l). By contrast, only 6 of 113 pre-$BCR^-$ ALL cases had $IC_{50}$<50 nmol/l and the vast majority of these cases did not respond to Dasatinib at concentrations up to 1,000 nmol/l (Figure 8B). Based on a large data set from 135 patient-derived ALL samples, we conclude that Dasatinib has strong selective anti-leukemia effects on pre-$BCR^+$ ALL cases. To confirm efficacy of Dasatinib *in vivo*, we transplanted leukemia cells from 4 patients with pre-$BCR^+$ ALL into sublethally irradiated NOD/SCID mice. Three of these cases carried a *TCF3-PBX1* gene rearrangement, and 1 case is hypodiploid. In 1 case (07-112), treatment with Dasatinib alone was sufficient to eradicate ALL and to cure mouse transplant recipients, whereas vehicle-treated mice died within 130 days after injection (Figure 8C). In the 3 other cases, Dasatinib treatment significantly delayed leukemic expansion and prolonged overall survival of transplant recipient mice. A composite Kaplan-Meier analysis of the 4 cases, injected into a total of 25 mice per group showed a substantial benefit of Dasatinib treatment (p=0.0001, Figure 8C). To monitor expansion of human leukemia cells (expressing human CD19 and CD45) in the recipient mice, peripheral blood from these mice was drawn weekly and analyzed for chimerism. The Dasatinib-treated cohorts showed minimal signs of circulating human chimerism comparing to the untreated cohorts (Figure 8C). These results demonstrate feasibility and efficacy of leukemia clearance *in vivo* of pre-$BCR^+$ ALL by Dasatinib based on 4 patient-derived samples. We expect that combinations with other pre-BCR signaling inhibitors (e.g. PRT062607, Ibrutinib) may have synergistic effects, which will be the focus of future studies by our group.

## DISCUSSION

Recent analyses revealed that BCR-dependent B cell lymphomas can be divided based on tonic or chronic active BCR signaling (Davis et al., 2010; Rickert, 2013; Schmitz et al., 2012). Tonic BCR signaling involves activation of one single pathway, namely PI3Kδ signaling downstream of SRC (LYN, FYN, BLK) and SYK (Burger and Okkenhaug, 2014; Chen et al., 2013), and is associated with germinal center B cell-like (GCB-) DLBCL and Burkitt's lymphoma (Young and Staudt, 2014). On the other hand, chronic active BCR signaling in ABC-DLBCL, CLL and MCL engages multiple downstream pathways including BTK (and its downstream targets PKCβ, MALT1 and NF-κB), calcineurin/NFAT and MEK/Erk (Young and Staudt, 2014). While the majority of B cell lymphoma cases are BCR-dependent and sensitive to BCR signaling antagonists, classical Hodgkin's lymphoma (Kanzler et al., 1996) and PMBL (Leithauser et al., 2001) together account for 15–20% of

human B cell lymphoma and lack BCR function. The classification of B cell lymphoma based on (i) chronic active, (ii) tonic and (iii) lack of BCR signaling informed the development of new treatment strategies and has led to the successful introduction of BTK (chronic active) (Byrd et al., 2013; Byrd et al., 2014; Wang et al., 2011) and PI3Kδ (tonic BCR signaling) inhibitors (Gopal et al., 2013) into patient care.

Like mature B cell lymphoma, pre-B ALL originates from B cell precursors that critically depend on survival signals emanating from a functional (pre-)BCR. In contrast to B cell lymphoma, however, a classification of human ALL based on pre-BCR function and activity is not available. Studying 830 ALL cases from four clinical trials, we found no functional equivalent of chronic active BCR signaling in B cell lymphoma. In the majority of ALL cases, ALL cells lacked pre-BCR signaling (pre-BCR$^-$), a functional equivalent to classical Hodgkin's lymphoma and PBML among mature B cell malignancies. However, in about 13.5% of human ALL cases, ALL cells expressed a functional pre-BCR (pre-BCR$^+$), and were highly sensitive to inhibition of SYK and SRC kinases and relatively resistant to inhibition of PKCβ, MALT1 and IKK/NF-κB.

Unlike ABC-DLBCL (chronic active BCR signaling), GCB-DLBCL express high levels of BCL6 in the context of tonic BCR signaling (Juszczynski et al., 2009). Here we found constitutive and pre-BCR-dependent expression of BCL6 in all pre-BCR$^+$ ALL cases studied. Conversely, as a marker in immunohistochemistry staining, BCL6 reliably identified pre-BCR$^+$ ALL cases. BCL6 expression is indeed dependent on tonic pre-BCR signaling, as small molecule inhibition of SYK and SRC family kinases abolished BCL6 expression in pre-BCR$^+$ ALL cells. Since functional assays to measure tonic pre-BCR signaling in ALL patient samples may not be practical for diagnostic purposes, we propose that BCL6 and μHC immunostaining may be a feasible alternative to rapidly identify patients that might benefit from treatment with inhibitors of tonic pre-BCR signaling (e.g. SYK, SRC, PIK3δ).

## EXPERIMENTAL PROCEDURES

### Primary Human Samples and Cell Lines

Primary ALL cases were obtained with the approval of the Institutional Review Boards of the University of California San Francisco (UCSF) and Oregon Health and Science University (OHSU). Primary human ALL samples were cultured on OP9 stroma in Minimum Essential Medium (MEMα, Life Technologies) with GlutaMAX containing 20% FBS, 100 IU ml$^{-1}$ penicillin, 100 μg ml$^{-1}$ streptomycin and 1mM sodium pyruvate at 37°C in a humidified incubator with 5% $CO_2$. The human cell lines were purchased from DSMZ (Braunschweig, Germany). See Table S1–S3.

### In Vivo Leukemia Cell Transplantation and Treatment

All mouse experiments were subject to institutional approval by the University of California San Francisco Institutional Animal Care and Use Committee. $10^6$ cells from primary *TCF3-PBX1* pre-BCR$^+$ ALL were inoculated via intravenous injection into sublethally irradiated (250 cGy) adult female NOD/SCID mice (n=28). After injection of leukemia cells, the mice

were randomly separated into 4 groups and treated with 1) Dasatinib (40 mg/kg); 2) Ibrutinib (75 mg/kg); 3) PRT062607 (100 mg/kg); 4) vehicle. Leukemic infiltration was confirmed by flow cytometry and bioimaging.

### Statistical Analysis

The Kaplan-Meier method was used to estimate overall survival. Log-rank test was used to compare survival differences between patient groups. The R package 'survival' version 2.35–8 was used for the survival analysis.

## Supplementary Material

Refer to Web version on PubMed Central for supplementary material.

## Acknowledgments

We thank Michael L Cleary (Stanford) for critical discussions, Arthur L Shaffer and Louis M Staudt for inducible BCL6 constructs, Mark Kamps and David B. Sykes for inducible *TCF3-PBX1* vectors, Lothar Hennighausen for *Stat5ab*$^{fl/fl}$ mice, and Julia Gastier-Foster and I-Ming Chen for fresh samples from the COG ALL Biology Bank (proposal #2008-08). This work is supported by grants from the NIH/NCI through R01CA137060, R01CA139032, R01CA157644, R01CA169458, R01CA172558 (to M.M.), CA178765 (to R.G.R.), R00CA151457 and R01CA183947 (to J.W.T.), U10 CA98543 (COG Chair's grant), U10 CA98413 (COG Statistical Center), and U24 CA114766 (COG Specimen Banking), the Hyundai Hope on Wheels, the St. Baldrick's Foundation, the Leukemia & Lymphoma Society Specialized Center of Research (LLS SCOR) and Tucker's Toy Box Foundation (to B.H.C.), the William Lawrence and Blanche Hughes Foundation, the California Institute for Regenerative Medicine (CIRM; TR2-01816), Leukaemia and Lymphoma Research (to M.M.), the Medical Research Council (UK) and the National Institute for Health Research Oxford Biomedical Research Centre Program (to T.M. and E.B). B.J.D. is supported by the Howard Hughes Medical Institute. M.M. is a Scholar of the Leukemia and Lymphoma Society and a Senior Investigator of the Wellcome Trust.

## References

Bayly R, Chuen L, Currie RA, Hyndman BD, Casselman R, Blobel GA, LeBrun DP. E2A-PBX1 interacts directly with the KIX domain of CBP/p300 in the induction of proliferation in primary hematopoietic cells. J Biol Chem. 2004; 279:55362–55371. [PubMed: 15507449]

Burger JA, Okkenhaug K. Haematological cancer: idelalisib-targeting PI3Kdelta in patients with B-cell malignancies. Nat Rev Clin Oncol. 2014; 11:184–186. [PubMed: 24642682]

Byrd JC, Furman RR, Coutre SE, Flinn IW, Burger JA, Blum KA, Grant B, Sharman JP, Coleman M, Wierda WG, et al. Targeting BTK with ibrutinib in relapsed chronic lymphocytic leukemia. N Engl J Med. 2013; 369:32–42. [PubMed: 23782158]

Byrd JC, O'Brien S, James DF. Ibrutinib in relapsed chronic lymphocytic leukemia. N Engl J Med. 2014; 369:1278–1279. [PubMed: 24066758]

Cerchietti LC, Yang SN, Shaknovich R, Hatzi K, Polo JM, Chadburn A, Dowdy SF, Melnick A. A peptomimetic inhibitor of BCL6 with potent antilymphoma effects in vitro and in vivo. Blood. 2009; 113:3397–3405. [PubMed: 18927431]

Chen L, Monti S, Juszczynski P, Ouyang J, Chapuy B, Neuberg D, Doench JG, Bogusz AM, Habermann TM, Dogan A, et al. SYK inhibition modulates distinct PI3K - dependent survival pathways and cholesterol biosynthesis in diffuse large B cell lymphomas. Cancer Cell. 2013; 23:826–838. [PubMed: 23764004]

Chen L, Juszczynski P, Takeyama K, Aguiar RC, Shipp MA. Protein tyrosine phosphatase receptor-type O truncated (PTPROt) regulates SYK phosphorylation, proximal B-cell-receptor signaling, and cellular proliferation. Blood. 2006; 108:3428–3433. [PubMed: 16888096]

Cheng S, Coffey G, Zhang XH, Shaknovich R, Song Z, Lu P, Pandey A, Melnick AM, Sinha U, Wang YL. SYK inhibition and response prediction in diffuse large B-cell lymphoma. Blood. 2011; 118:6342–6352. [PubMed: 22025527]

Davis RE, Ngo VN, Lenz G, Tolar P, Young RM, Romesser PB, Kohlhammer H, Lamy L, Zhao H, Yang Y, et al. Chronic active B-cell-receptor signalling in diffuse large B-cell lymphoma. Nature. 2010; 463:88–92. [PubMed: 20054396]

Duy C, Hurtz C, Shojaee S, Cerchietti L, Geng H, Swaminathan S, Klemm L, Kweon SM, Nahar R, Braig M, et al. BCL6 enables Ph+ acute lymphoblastic leukaemia cells to survive BCR-ABL1 kinase inhibition. Nature. 2011; 473:384–388. [PubMed: 21593872]

Duy C, Yu JJ, Nahar R, Swaminathan S, Kweon SM, Polo JM, Valls E, Klemm L, Shojaee S, Cerchietti L, et al. BCL6 is critical for the development of a diverse primary B cell repertoire. J Exp Med. 2010; 207:1209–1221. [PubMed: 20498019]

Geng H, Brennan S, Milne TA, Chen WY, Li Y, Hurtz C, Kweon SM, Zickl L, Shojaee S, Neuberg D, et al. Integrative Epigenomic Analysis Identifies Biomarkers and Therapeutic Targets in Adult B-Acute Lymphoblastic Leukemia. Cancer Discov. 2012; 2:1004–1023. [PubMed: 23107779]

Gopal AK, Kahl BS, de Vos S, Wagner-Johnston ND, Schuster SJ, Jurczak WJ, Flinn IW, Flowers CR, Martin P, Viardot A, et al. PI3Kdelta inhibition by idelalisib in patients with relapsed indolent lymphoma. N Engl J Med. 2013; 370:1008–1018. [PubMed: 24450858]

Guo B, Kato RM, Garcia-Lloret M, Wahl MI, Rawlings DJ. Engagement of the human pre-B cell receptor generates a lipid raft-dependent signaling complex. Immunity. 2000; 13:243–253. [PubMed: 10981967]

Harvey RC, Mullighan CG, Wang X, Dobbin KK, Davidson GS, Bedrick EJ, Chen IM, Atlas SR, Kang H, Ar K, et al. Identification of novel cluster groups in pediatric high-risk B-precursor acute lymphoblastic leukemia with gene expression profiling: correlation with genome-wide DNA copy number alterations, clinical characteristics, and outcome. Blood. 2010; 116:4874–4884. [PubMed: 20699438]

Juszczynski P, Chen L, O'Donnell E, Polo JM, Ranuncolo SM, Dalla-Favera R, Melnick A, Shipp MA. BCL6 modulates tonic BCR signaling in diffuse large B-cell lymphomas by repressing the SYK phosphatase, PTPROt. Blood. 2009; 114:5315–5321. [PubMed: 19855081]

Kanzler H, Kuppers R, Hansmann ML, Rajewsky K. Hodgkin and Reed-Sternberg cells in Hodgkin's disease represent the outgrowth of a dominant tumor clone derived from (crippled) germinal center B cells. J Exp Med. 1996; 184:1495–1505. [PubMed: 8879220]

Ke J, Chelvarajan RL, Sindhava V, Robertson DA, Lekakis L, Jennings CD, Bondada S. Anomalous constitutive Src kinase activity promotes B lymphoma survival and growth. Mol Cancer. 2009; 8:132. [PubMed: 20043832]

Kraus M, Alimzhanov MB, Rajewsky N, Rajewsky K. Survival of resting mature B lymphocytes depends on BCR signaling via the Igalpha/beta heterodimer. Cell. 2004; 117:787–800. [PubMed: 15186779]

Leithauser F, Bauerle M, Huynh MQ, Moller P. Isotype-switched immunoglobulin genes with a high load of somatic hypermutation and lack of ongoing mutational activity are prevalent in mediastinal B-cell lymphoma. Blood. 2001; 98:2762–2770. [PubMed: 11675349]

Nourse J, Mellentin JD, Galili N, Wilkinson J, Stanbridge E, Smith SD, Cleary ML. Chromosomal translocation t(1;19) results in synthesis of a homeobox fusion mRNA that codes for a potential chimeric transcription factor. Cell. 1990; 60:535–545. [PubMed: 1967982]

Ochiai K, Maienschein-Cline M, Mandal M, Triggs JR, Bertolino E, Sciammas R, Dinner AR, Clark MR, Singh H. A self-reinforcing regulatory network triggered by limiting IL-7 activates pre-BCR signaling and differentiation. Nat Immunol. 2012; 13:300–307. [PubMed: 22267219]

Okada T, Maeda A, Iwamatsu A, Gotoh K, Kurosaki T. BCAP: the tyrosine kinase substrate that connects B cell receptor to phosphoinositide 3-kinase activation. Immunity. 2000; 13:817–827. [PubMed: 11163197]

Osmond DG. Proliferation kinetics and the lifespan of B cells in central and peripheral lymphoid organs. Curr Opin Immunol. 1991; 3:179–185. [PubMed: 2069745]

Rajewsky K. Clonal selection and learning in the antibody system. Nature. 1996; 381:751–758. [PubMed: 8657279]

Ramadani F, Bolland DJ, Garcon F, Emery JL, Vanhaesebroeck B, Corcoran AE, Okkenhaug K. The PI3K isoforms p110alpha and p110delta are essential for pre-B cell receptor signaling and B cell development. Sci Signal. 2010; 3:ra60. [PubMed: 20699475]

Rickert RC. New insights into pre-BCR and BCR signalling with relevance to B cell malignancies. Nat Rev Immunol. 2013; 13:578–591. [PubMed: 23883968]

Ross ME, Zhou X, Song G, Shurtleff SA, Girtman K, Williams WK, Liu HC, Mahfouz R, Raimondi SC, Lenny N, et al. Classification of pediatric acute lymphoblastic leukemia by gene expression profiling. Blood. 2003; 102:2951–2959. [PubMed: 12730115]

Saijo K, Schmedt C, Su IH, Karasuyama H, Lowell CA, Reth M, Adachi T, Patke A, Santana A, Tarakhovsky A. Essential role of Src-family protein tyrosine kinases in NF-kappaB activation during B cell development. Nat Immunol. 2003; 4:274–279. [PubMed: 12563261]

Sakaguchi N, Melchers F. Lambda 5, a new light-chain-related locus selectively expressed in pre-B lymphocytes. Nature. 1986; 324:579–582. [PubMed: 3024017]

Sanyal M, Tung JW, Karsunky H, Zeng H, Selleri L, Weissman IL, Herzenberg LA, Cleary ML. B-cell development fails in the absence of the Pbx1 proto-oncogene. Blood. 2007; 109:4191–4199. [PubMed: 17244677]

Schmitz R, Young RM, Ceribelli M, Jhavar S, Xiao W, Zhang M, Wright G, Shaffer AL, Hodson DJ, Buras E, et al. Burkitt lymphoma pathogenesis and therapeutic targets from structural and functional genomics. Nature. 2012; 490:116–120. [PubMed: 22885699]

Schweighoffer E, Vanes L, Mathiot A, Nakamura T, Tybulewicz VL. Unexpected requirement for ZAP-70 in pre-B cell development and allelic exclusion. Immunity. 2003; 18:523–533. [PubMed: 12705855]

Shaffer AL, Yu X, He Y, Boldrick J, Chan EP, Staudt LM. BCL-6 represses genes that function in lymphocyte differentiation, inflammation, and cell cycle control. Immunity. 2000; 13:199–212. [PubMed: 10981963]

Srinivasan L, Sasaki Y, Calado DP, Zhang B, Paik JH, DePinho RA, Kutok JL, Kearney JF, Otipoby KL, Rajewsky K. PI3 kinase signals BCR-dependent mature B cell survival. Cell. 2009; 139:573–586. [PubMed: 19879843]

Swaminathan S, Huang C, Geng H, Chen Z, Harvey R, Kang H, Ng C, Titz B, Hurtz C, Sadiyah MF, et al. BACH2 mediates negative selection and p53-dependent tumor suppression at the pre-B cell receptor checkpoint. Nat Med. 2013; 19:1014–1022. [PubMed: 23852341]

Tibes R, Qiu Y, Lu Y, Hennessy B, Andreeff M, Mills GB, Kornblau SM. Reverse phase protein array: validation of a novel proteomic technology and utility for analysis of primary leukemia specimens and hematopoietic stem cells. Mol Cancer Ther. 2006; 5:2512–2521. [PubMed: 17041095]

Trageser D, Iacobucci I, Nahar R, Duy C, von Levetzow G, Klemm L, Park E, Schuh W, Gruber T, Herzog S, et al. Pre-B cell receptor-mediated cell cycle arrest in Ph+ acute lymphoblastic leukemia requires IKAROS function. J Exp Med. 2009; 206:1739–1753. [PubMed: 19620627]

Tyner JW, Yang WF, Bankhead A 3rd, Fan G, Fletcher LB, Bryant J, Glover JM, Chang BH, Spurgeon SE, Fleming WH, et al. Kinase pathway dependence in primary human leukemias determined by rapid inhibitor screening. Cancer Res. 2013; 73:285–296. [PubMed: 23087056]

Wang L, Li L, Zhang H, Luo X, Dai J, Zhou S, Gu J, Zhu J, Atadja P, Lu C, et al. Structure of human SMYD2 protein reveals the basis of p53 tumor suppressor methylation. J Biol Chem. 2011; 286:38725–38737. [PubMed: 21880715]

Wang ML, Rule S, Martin P, Goy A, Auer R, Kahl BS, Jurczak W, Advani RH, Romaguera JE, Williams ME, et al. Targeting BTK with ibrutinib in relapsed or refractory mantle-cell lymphoma. N Engl J Med. 2013; 369:507–516. [PubMed: 23782157]

Yang C, Lu P, Lee FY, Chadburn A, Barrientos JC, Leonard JP, Ye F, Zhang D, Knowles DM, Wang YL. Tyrosine kinase inhibition in diffuse large B-cell lymphoma: molecular basis for antitumor activity and drug resistance of dasatinib. Leukemia. 2008; 22:1755–1766. [PubMed: 18596745]

Ye BH, Lista F, Lo Coco F, Knowles DM, Offit K, Chaganti RS, Dalla-Favera R. Alterations of a zinc finger-encoding gene, BCL-6, in diffuse large-cell lymphoma. Science. 1993; 262:747–750. [PubMed: 8235596]

Young RM, Staudt LM. Targeting pathological B cell receptor signalling in lymphoid malignancies. Nat Rev Drug Discov. 2014; 12:229–243. [PubMed: 23449308]

## HIGHLIGHTS

- ALL can be divided into two distinct subtypes based on pre-BCR function
- Pre-BCR-induced activation of BCL6 further increased pre-BCR signaling output
- Pre-BCR inhibitors reduced BCL6 levels and selectively killed pre-BCR$^+$ ALL cells
- BCL6 represents a biomarker to identify patients with pre-BCR$^+$ ALL

## SIGNIFICANCE

Recent work successfully introduced BCR signaling inhibitors into patient care for various subtypes of mature B cell lymphoma, e.g. Ibrutinib (BTK) and Idelalisib (PI3Kδ) for germinal center-derived B cell lymphoma. However, it is not known whether pre-BCR signaling represents a therapeutic target in pre-B ALL. Here we report the identification of a subset of human ALL cases that critically depend on tonic pre-BCR signaling and are selectively sensitive to small molecule inhibitors of SYK and SRC tyrosine kinases downstream of the pre-BCR.

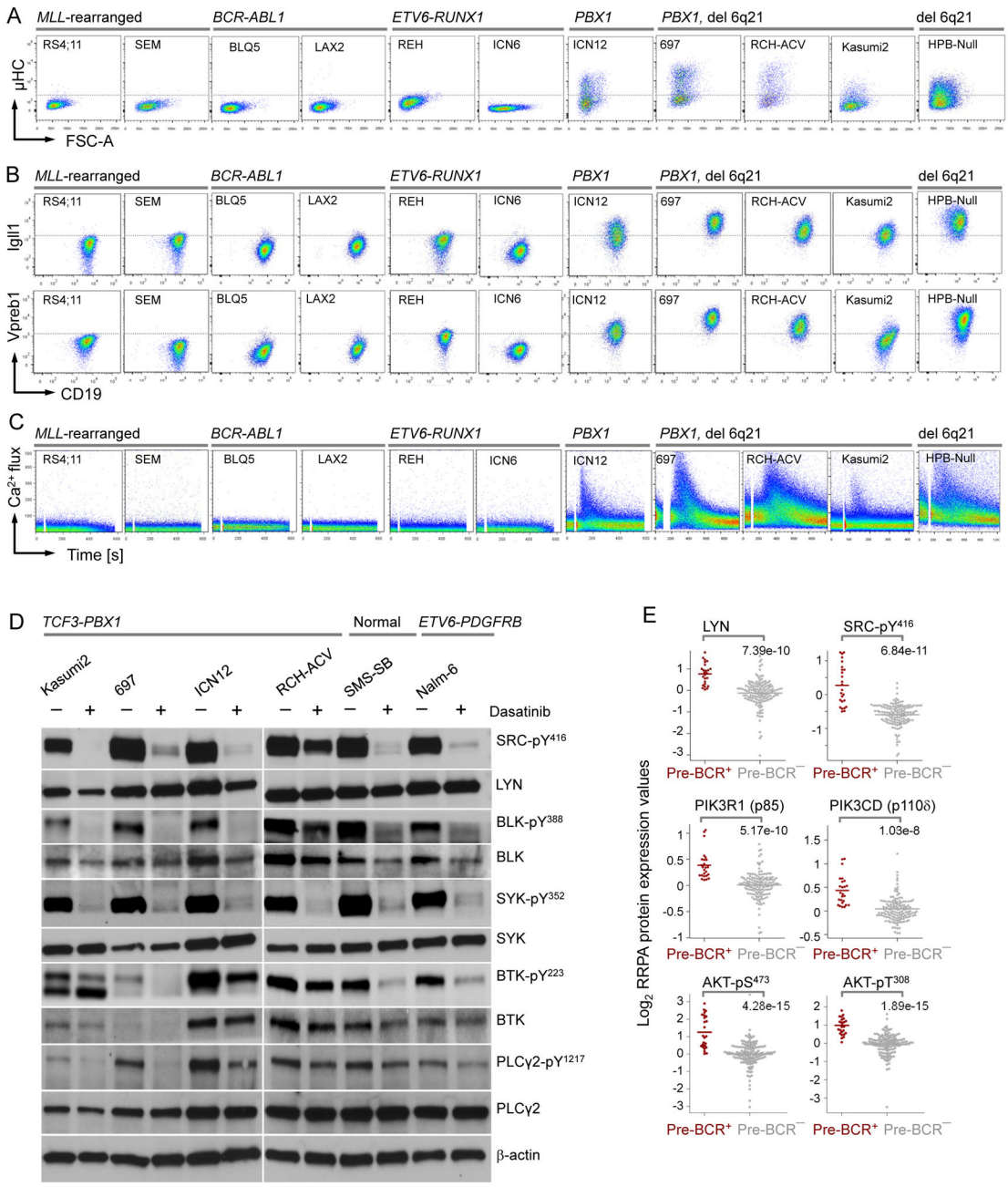


**Figure 1. Expression and Activity of the pre-BCR Receptor in Subsets of pre-B ALL**

(**A**) Flow cytometry staining for cell cytoplasmic μHC, (**B**) cell surface expression of the surrogate light chain components λ5 (IGLL1) and VpreB, and (**C**) $Ca^{2+}$ mobilization in response to pre–BCR engagement using μHC-specific antibodies in different subtypes of ALL cases. (**D**) Patient-derived Pre-BCR$^{+}$ ALL cells were treated with or without Dasatinib (25 μmol/l, 24 hr). Phosphorylation of SRC, BLK, SYK, BTK and PLCγ2 were measured by Western blot. (**E**) Protein expression and phosphorylation levels of LYN, SRC, PIK3R1 (p85), PIK3CD (p110δ) and AKT were measure by reverse phase protein arrays (RPPA) in pre-BCR$^{+}$ vs. pre-BCR$^{−}$ ALL patient samples (MDACC 1983–2007; n=208). Y axis shows

$log_2$ expression values of RPPA data. P values were calculated from two-sided Wilcoxon test. See also Figure S1 and Table S1–S3.

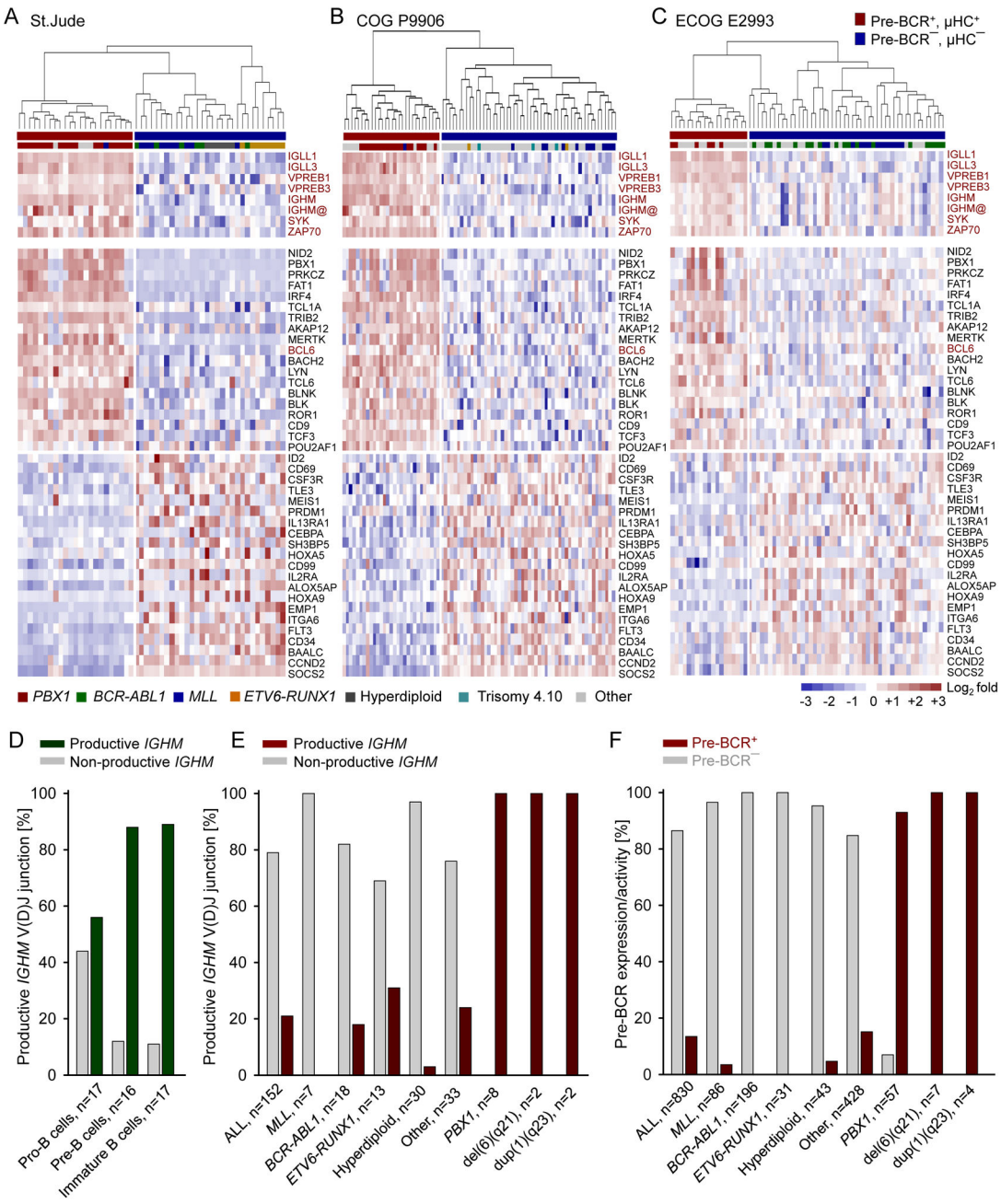


**Figure 2. Pre-BCR Signaling in ALL Is Associated with a Distinct Gene Expression and Signal Transduction Phenotype**

(**A–C**) Gene expression microarray data was analyzed from 3 cohorts of pre-B ALL patient samples for children (St. Jude Research Hospital; COG P9906) and adults (ECOG E2993). In each dataset, the patient samples were ranked based on their average mRNA expression levels of pre-BCR molecules (*IGLL1*, *IGLL3*, *VPREB1*, *VPREB3*, *IGHM*, *SYK* and *ZAP70*). The top 15% and the bottom 25% cases were considered as the pre-BCR$^{+}$ and pre-BCR$^{-}$ and subject to the clustering analysis. Supervised analysis on pre-BCR$^{+}$ vs. pre-BCR$^{-}$ ALL revealed a 40-gene expression signature that is significantly up- or down-regulated across all

3 cohorts. The color scale bar represents the relative $\log_2$ expression changes. (**D**) The configuration of the μ heavy chain locus (*IGHM*) was studied in human bone marrow pro-, pre- and immature B cells and (**E**) different subtypes of ALL patient samples (n=152). Y axis shows frequencies of normal B-cells or ALL clones with a functional or a non-functional *IGHM* gene rearrangement in these populations. (**F**) Frequency of different cytogenetic subtypes of pre-B ALL cases as pre-$BCR^+$ or pre-$BCR^-$ based on 4clinical trials (n=830, MDACC, St. Jude, COG and ECOG). See also Table S4–S6.

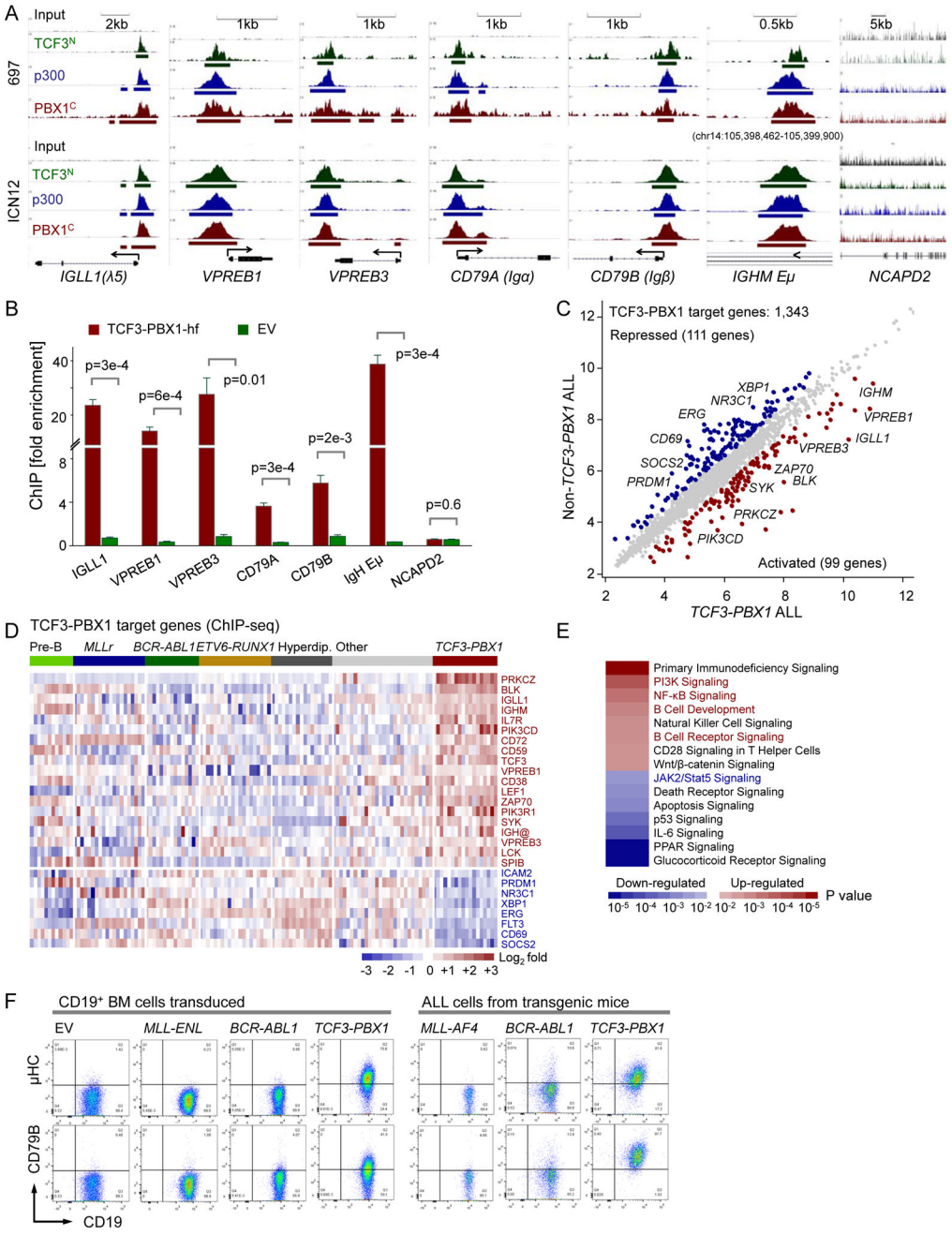


**Figure 3. TCF3-PBX1 fusion protein binds to and upregulates genes encoding pre-BCR components**

(**A**) ChIPseq tracks for TCF3$^{N}$, PBX1$^{C}$ and p300 antibodies vs. input in a *TCF3-PBX1* ALL line 697 and a primary sample ICN12 on *IGLL1*, *VPREB1*, *VPREB3*, *CD79A* and *CD79B* promoter regions and the *IGHM* enhancer regions *(Eμ)*. Gene models were shown in UCSC genome browser hg18. **B** () QChIP validation using an HA antibody that is specific for the HA-Flag-tagged *TCF3-PBX1* fusion or an EV as control. *NCAPD2* serves as a negative control gene. Data represent means ± SEM (n=3). P values from t-test. (**C**) The scatter plot shows the average gene expression values of the *TCF3-PBX1-rearranged* (x-axis) vs. the

non-*TCF3-PBX1-rearranged* ALL patient samples (y-axis) from the St. Jude dataset on the *TCF3-PBX1* target genes (n=1,343). Blue and red highlighted are the down- (n=111) and up- (n=99) regulated genes (>1.5 fold change). (**D**) The heatmap representation for some up- or down-regulated genes. The color scale bar represents the $\log_2$ expression changes. (**E**) Ingenuity pathway analysis for the up- and down-regulated genes. The color scale indicates p values calculated from Ingenuity. (**F**). Flow cytometry staining for cytoplasmic μHC, surface CD79B and CD19 in full-blown ALL populations that had developed after latencies of 90–180 days in the bone marrow from the *MLL-AF4-*, *BCR-ABL1-* or *TCF3-PBX1-* transgenic mice. See also Figure S2.

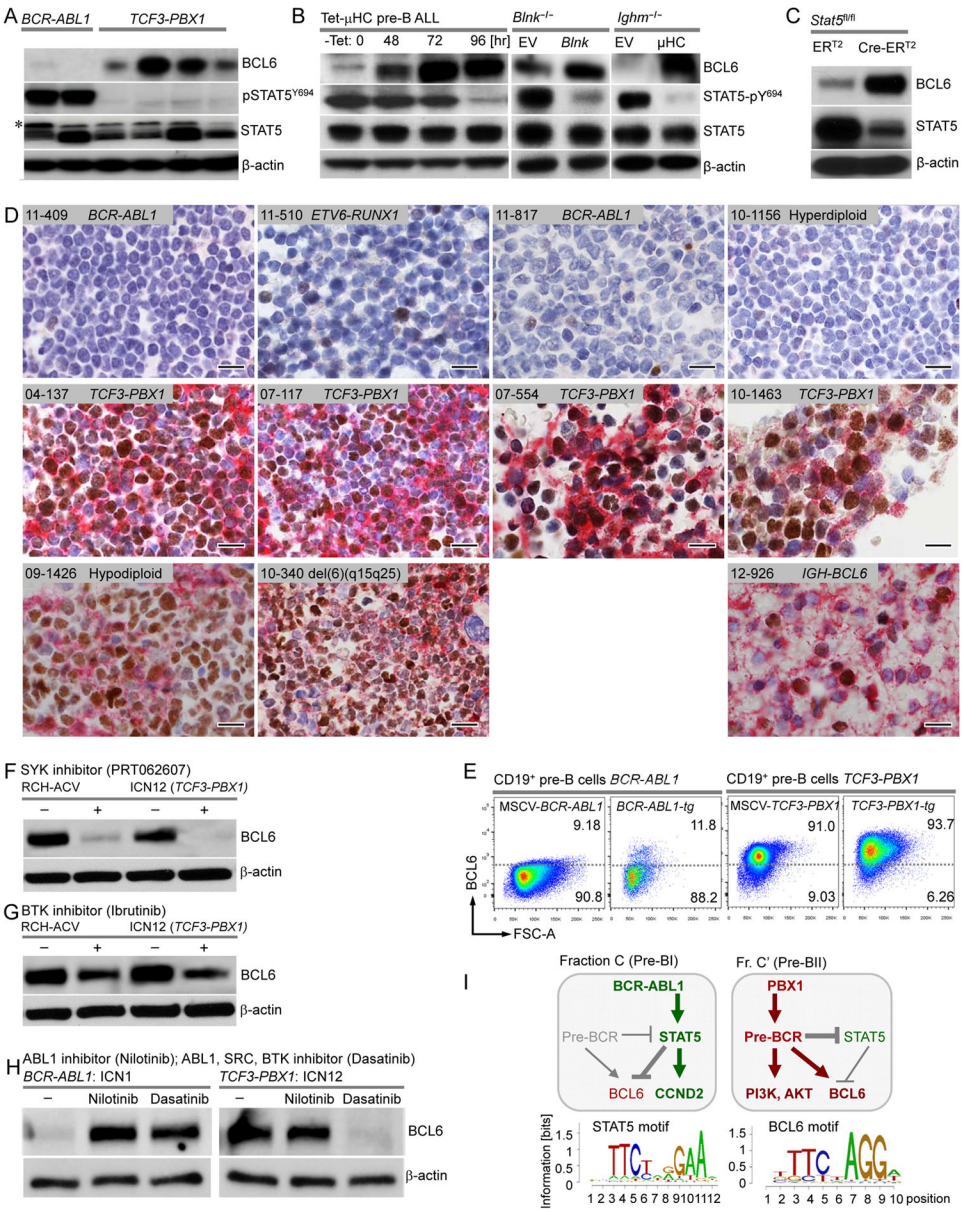


**Figure 4. Pre-BCR Signaling in ALL Cells Drives Expression of BCL6**

(**A**) BCL6, STAT5, and pSTAT5$^{Y694}$ Western blotting with β-actin as a loading control in human *BCR-ABL1* or *TCF3-PBX1* ALL samples. Asterisk denotes non-specific band. (**B**) Protein expression levels of BCL6, STAT5 and pSTAT5$^{Y694}$ by Western blot with β-actin as the loading control at different time points of tetracycline culture of Rag2$^{-/-}$ tTA/μ-chain ALL cells (*left* panel), before and after pre-BCR signaling reconstitution by retroviral expression of Blnk-GFP or GFP EV in the *Blnk*$^{-/-}$ ALL cells (*middle* panel), or CD8/μ-chain or CD8 EV in *Ighm*$^{-/-}$ ALL cells (*right* panel). (**C**) BCL6 and STAT5 Western blot in the presence or absence of Cre-mediated deletion of *Stat5* in Stat5$^{fl/fl}$ pre-B ALL cells. (**D**) Immunohistochemistry double-stainings for BCL6 (nuclear, brown) and μHC (cytoplasmic/membrane, red) on the same slides of paraffin-embedded bone marrow samples from Pre-

$BCR^-$ and Pre-$BCR^+$ ALL patients. A Burkitt's lymphoma sample (12-926) carrying an *IGH-BCL6* gene rearrangement was used as a positive control. Scale bars, 20 um. (**E**) Bone marrow pre-B cells transduced with *BCR-ABL1* or *TCF3-PBX1* vectors, or from full-blown ALL populations that had developed after latencies of 90–180 days from the *BCR-ABL1*- or *TCF3-PBX1*-transgenic mice were stained for intracellular Bcl6 protein. Cells were gated as live CD19+ cells. The Bcl6 expression threshold was set according to an isotype staining control. (**F–G**) BCL6 protein expression by Western blotting in presence or absence of SYK inhibitor (PRT062607, 10 μmol/l), BTK inhibitor (Ibrutinib, 10 μmol/l) for 24 hr in a *TCF3-PBX1* ALL cell line (RCH-ACV) and a primary sample (ICN12), or (**H**) in presence or absence of Nilotinib (200 nmol/l) or Dasatinib (25 nmol/l) for 24 hr in primary *BCR-ABL1* (ICN1) or *TCF3-PBX1* (ICN12) ALL cells. β-actin was used as a loading control. (**I**) A schematic of pre-BCR, STAT5 and BCL6 regulation in *BCR-ABL1* and *TCF3-PBX1* ALL. See also Figure S3 and Table S7-S8.

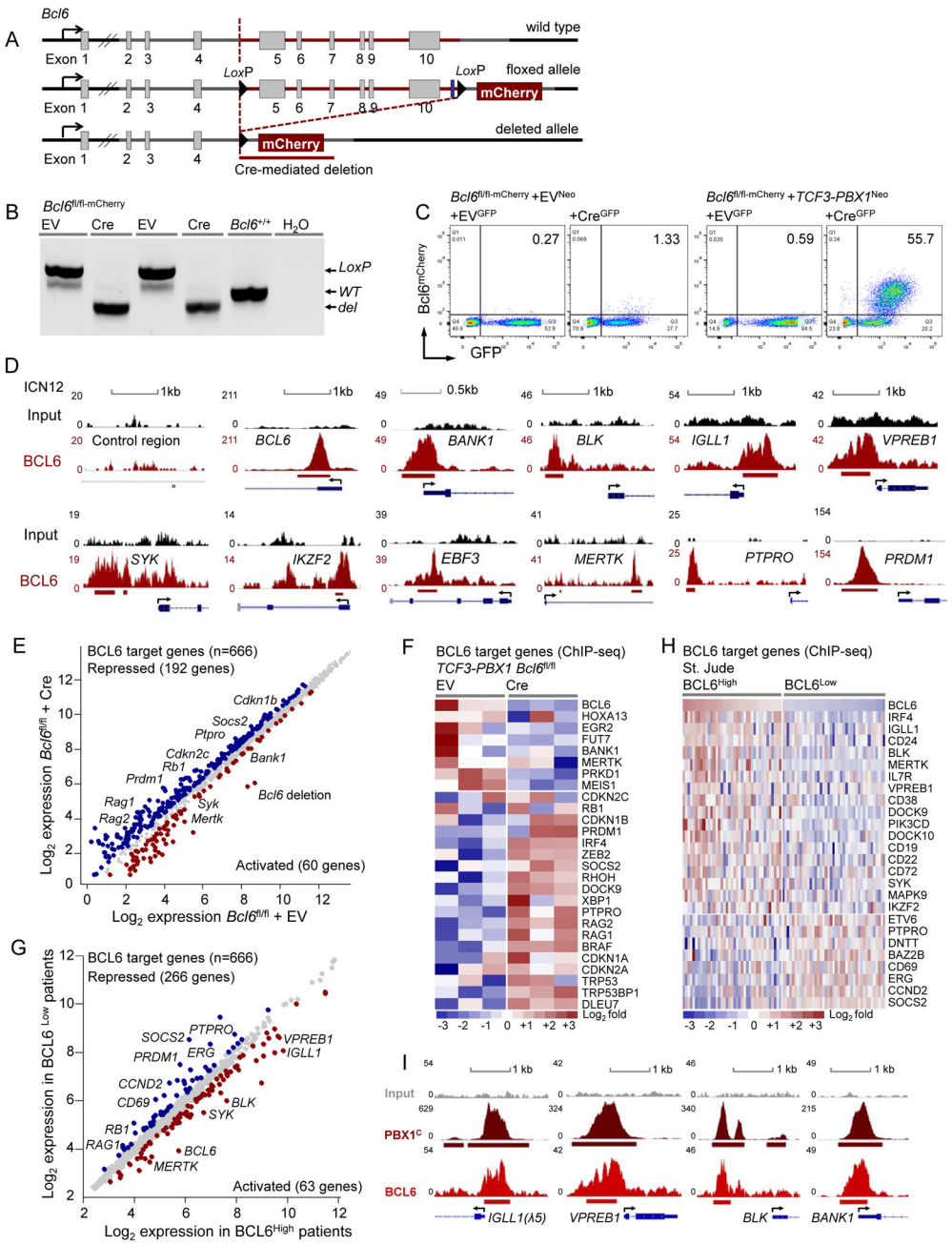


**Figure 5. BCL6 Is a Key Regulator of the Transcriptional Program in pre-BCR$^+$ ALL Cells**

(**A**) A genetic model for inducible ablation of *BCL6* and a mCherry-based Bcl6 reporter (*Bcl6*$^{fl/fl}$-mCherry). Exons 5–10 of the *Bcl6* locus were targeted for inducible Cre-mediated deletion. *LoxP* sites are indicated as black triangles. (**B**) PCR validation of the floxed, deleted and wild type *Bcl6* allele from *Bcl6*$^{fl/fl}$-mCherry mouse bone marrow pre-B cells. (**C**) FACS analysis of EV$^{Neo}$ or *TCF3-PBX1*$^{Neo}$ retrovirally transduced *Bcl6*$^{fl/fl}$-mCherry pre-B cells that were transduced with either EV$^{GFP}$ or Cre$^{GFP}$ vector for *Bcl6* deletion. Y-axis indicates mCherry expression and x-axis indicates GFP expression. (**D**) BCL6 ChIPseq binding tracks of target genes in patient-derived *TCF3-PBX1* ALL cells (ICN12). Y axis

represents the number of reads for peak summit normalized by the total number of reads per track. Gene models are shown in UCSC genome browser hg18. A control intragenic region and BCL6 were used as negative and positive controls. (**E–F**) A meta-analysis of BCL6 ChIPseq target genes (n=666) with gene expression microarray data for the EV vs. Cre transduced *Bcl6*$^{fl/fl}$ *TCF3-PBX1* ALL cells or (**G–H**) for the BCL6$^{High}$ vs. BCL6$^{Low}$ ALL patient samples from St. Jude. The scatter or heatmap plots showed up- and down-regulated BCL6 target genes in each data set. The color scale bar represents relative $\log_2$ expression changes. (**I**) PBX1 and BCL6 ChIPseq binding tracks vs. input in ICN12 cells on pre-BCR-related genes (*IGLL1*, *VPREB1*, *BLK*, *BANK1*). See also Figure S4.

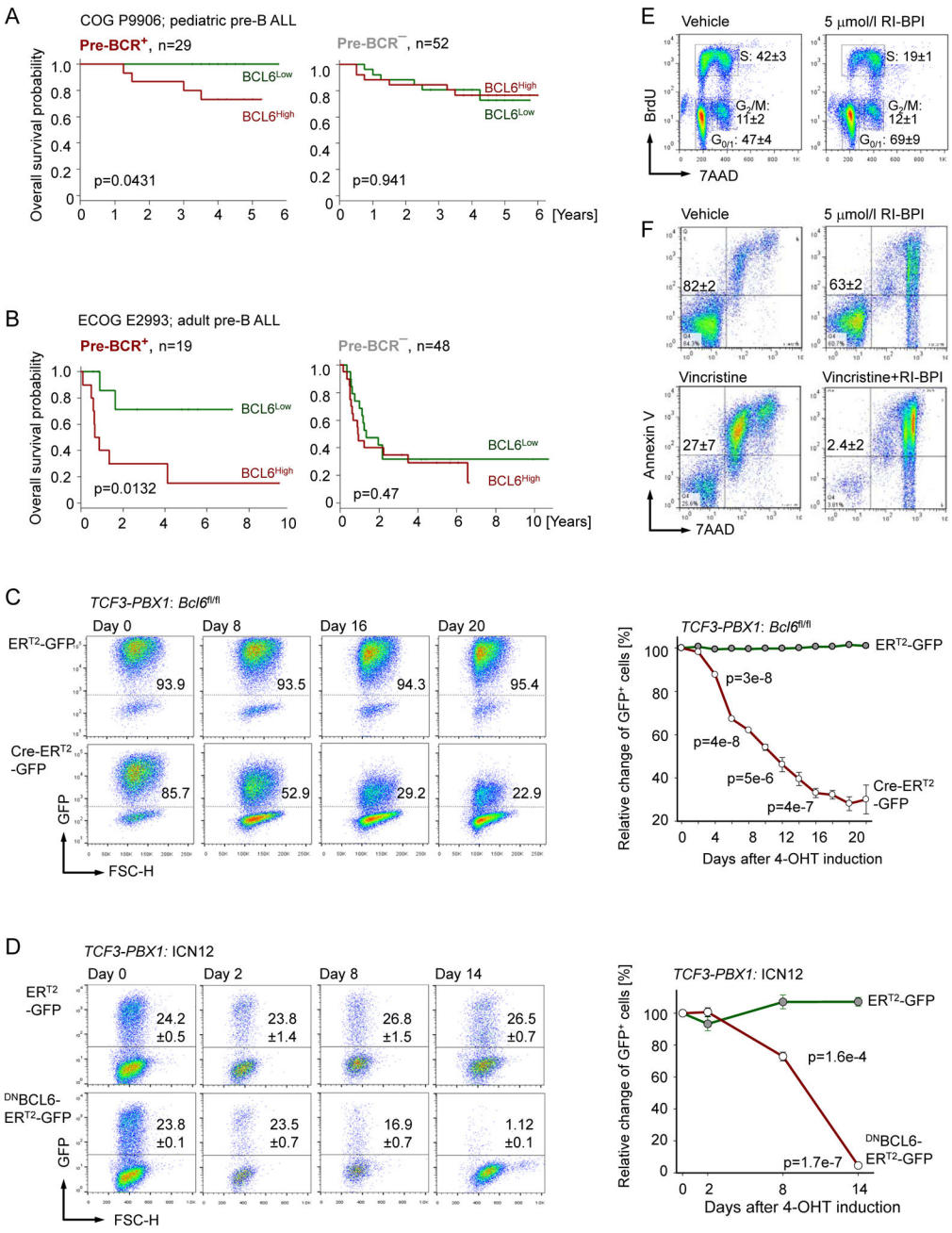


**Figure 6. Pre-BCR$^+$ ALL Cells Are Dependent on BCL6-Activity**

(**A–B**) Patients were segregated into two groups based on higher or lower than the median expression of BCL6 in pre-BCR$^+$ and pre-BCR$^-$ ALL in 2 clinical trials: (**A**) COG P9906 and (**B**) ECOG E2993. Kaplan-Myer estimates were used to plot the survival probabilities. P values were calculated from the log-rank test. (**C**) *Bcl6*$^{fl/fl}$ *TCF3-PBX1* pre-B ALL cells were transduced with 4-OHT-inducible Cre (Cre-ER$^{T2}$-GFP) or EV control (ER$^{T2}$-GFP). Percentage of GFP-positive cells were measure by flow cytometry at different time points following 4-OHT treatment and time course data are depicted. (**D**) Patient-derive Pre-BCR$^+$ ALL cells (ICN12) were transduced with 4-OHT-inducible dominant-negative BCL6

($^{DN}$BCL6-ER$^{T2}$-GFP) or EV control (ER$^{T2}$-GFP). Percentages of GFP-positive cells were measured by the flow cytometry at different time points following 4-OHT treatment. (**E**) ICN12 cells were treated with vehicle or 5 μmol/l RI-BPI for 24 hr and then subjected to cell-cycle analysis (BrdU and 7-AAD staining). (**F**) ICN12 cells were exposed to vehicle, Vincristine (1 nmol/l), RI-BPI (5 μmol/l), or combination of Vincristine (1 nmol/l) and RI-BPI (5 μmol/l) for 3 days, followed by flow cytometry for Annexin V and 7-AAD staining. Data represent means ± SEM (n=3). P values from t-test. See also Figure S5.

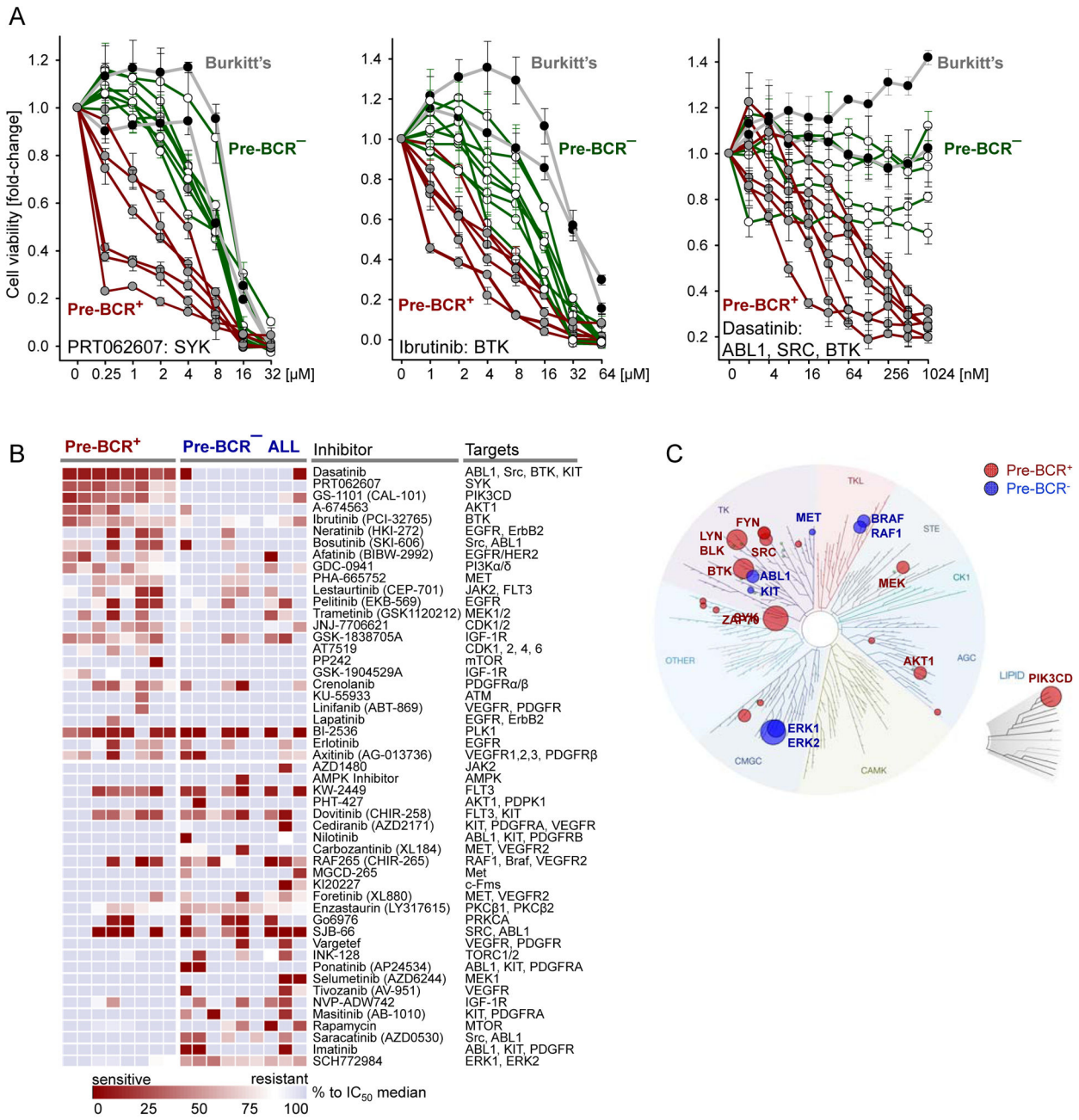


**Figure 7. Validation of Pharmacological Inhibition of BCL6-pre-BCR Signaling as Therapeutic Target in pre-BCR$^+$ ALL Cells**

(**A**) Cell viability was measured using CCK-8 in presence or absence of PRT062607 (SYK), Ibrutinib (BTK) or Dasatinib (ABL1/SRC/BTK) for 72 hr with gradients of concentrations as indicated in the X axis in pre-BCR$^+$ ALL (n=7), pre-BCR$^-$ ALL (n=8) and 2 Burkitt lymphoma (MN60, MHH-preB). Y axis shows the percentage of viable cells with the untreated cells as control (set to 100%). Data represent means ± SD (n=3). (**B**) Pre-BCR$^+$ (n=8) and pre-BCR$^-$ (n=9) patient-derived ALL samples were treated with a diverse panel of 51 kinase inhibitors as described previously (Tyner et al., 2013). The heatmap represents

the $IC_{50}$ values for each sample relative to the observed median $IC_{50}$ value for over 400 primary leukemia samples interrogated by this assay at OHSU. Red or blue colors denote higher or lower than the median sensitivity of the pre-B ALL cells tested. Pre-$BCR^+$ ALL: 07-112, 11-064, ICN12, 697, RCH-ACV, Kasumi-2, HPB-null, Nalm6. Pre-$BCR^-$ ALL: BV173, SUPB15, BLQ5, LAX2, SEM, RS4;11, REH, LAX7R, SFO3. (**C**) Kinase dendrogram of pre-$BCR^+$ and pre-$BCR^-$ ALL based on experimentally measured sensitivities to individual inhibitors and their known inhibitory profile based on biochemical $IC_{50}$ values for individual kinase targets. TREESpots software was used (KINOMEscan, http://www.discoverx.com/). See also Figure S6.

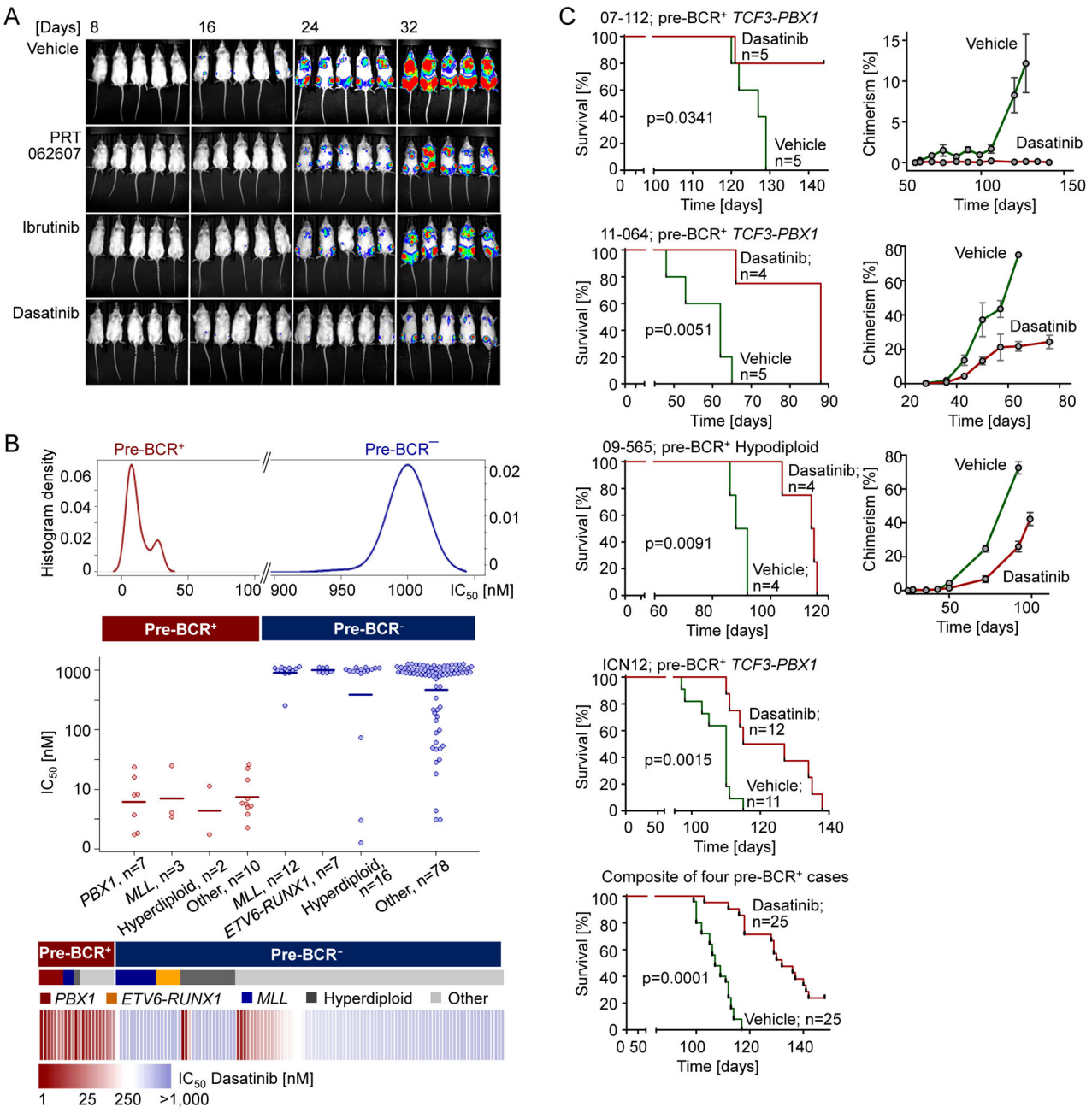


**Figure 8. Validation of Pharmacological Inhibition of BCL6-pre-BCR Signaling in Patient-Derived pre-BCR$^+$ ALL Cells**

(**A**) Patient-derived pre-BCR$^+$ ALL cells (ICN12) were labelled with luciferase and 1,000,000 cells were injected intravenously to sublethally irradiated NOD/SCID mice. The mice were randomly separated into 4 groups and treated with vehicle, the SYK inhibitor PRT062607 (100 mg/kg), the BTK inhibitor Ibrutinib (75 mg/kg), or Dasatinib (40 mg/kg) respectively. Bioimages were taken at different time points for each of the groups. (**B**) Plot of Dasatinib $IC_{50}$'s from primary ALL patient samples (n=135, OHSU). ALL samples were cultured over 72 hr in the presence or absence of Dasatinib in concentrations ranging from 1

nmol/l to 1,000 nmol/l to calculate the $IC_{50}$ values. (**C**) Patient-derived pre-$BCR^+$ ALL cells (n=4) were injected to sublethally irradiated NOD/SCID mice. Mice were treated with vehicle or Dasatinib (40–50 mg/kg). Kaplan-Meier estimates were used to plot the survival probabilities for each treatment group vs. vehicle control. P values were calculated from log-rank test. Peripheral blood was drawn weekly and analyzed for chimerism with either human CD19 or human CD45 vs. murine CD45 and plotted over time. Data represent means ± SD (n=4 or 5).